Design of Optimal Cancer Chemotherapy Using a Continuous-Time State Model of Cell Kinetics

KANG G. SHIN AND RICHARD PADO
Electrical, Computer and Systems Engineering Department, Rensselaer Polytechnic Institute, Troy, New York 12181

Received 4 August 1981; revised 19 November 1981

ABSTRACT

A continuous bilinear model in state space is used to describe the cell kinetics of a tumor-cell population under the effects of chemotherapy. Firstly, the time-course behavior of a Chinese-hamster-ovary (CHO) cell population is simulated to demonstrate the utility of the model. Then, an optimal strategy for cancer treatment is derived, based on the need to balance the effects on both cancerous and normal tissues. The performance index minimized is the sum of the weighted tumor population and the weighted total drug dosage. The optimization problem has resulted in a two-point boundary-value problem (TPBVP) with a bang-bang control policy, which is solved by the switching-time variation method (STVM). Computer simulation of CHO cells is also carried out as a numerical example of determining optimal cancer chemotherapy.

I. INTRODUCTION

Most of existing chemotherapeutic agents are known to damage both cancerous and normal tissues somewhat indiscriminately. For this reason, chemotherapy and radiotherapy have particularly harsh effects on renewing tissues such as hair, bone marrow, and the gastrointestinal lining. It is thus necessary to establish strategies which do maximal damage to cancerous tissues with only moderate damage to normal tissues. Consequently, the idea of an optimal control strategy is particularly relevant.

Differences in the susceptibility of tumor cells to antitumor agents have been shown most clearly as a function of their positions in the cell cycle. Thus the study of cell kinetics, the quantitative description of actively growing cell populations, can vastly improve the efficacy of chemotherapy.

A number of mathematical models have been proposed to describe the progression of proliferating cells through the cell cycle (for a review, see [1]), particularly for cell cultures and untreated cell populations. Based on these models, the effects of drugs have also been described quantitatively [2–3]. All of these models either have been unrealistically simple or have not been fully developed due to the lack of quantitative data, which are now beginning to be generated abundantly by the wide use of flow-microfluorometry (FMF)

52 Vanderbilt Ave., New York, NY 10017 0025-5564/82/04255+24$02.75

devices [4–6]. It is now appropriate to further develop theoretical cell-kinetic models and to derive the best treatment strategies.

Kim et al. [7] have developed cell-kinetic models by modifying the discrete-time, state-vector approach of Hahn [8] to include output equations for the cell size and DNA distributions, which are the standard measurements. These models contain multiple compartments, thus describing cell movements through the cell cycle more accurately than others dealing with only total populations or small numbers of subpopulations. They have also added control functions for the cancer treatment, and have described how to estimate the cell-kinetic parameters [9–11].

The above mathematical models can be used in predicting the response of a cell population to treatment and in determining the optimal dosage levels and intervals of the treatment. Swan and Vincent [12] derived a solution minimizing the total amount of cytotoxic drug in the host subject to an exponential equation relating total population and time; cell phases were not considered. Almquist and Banks [13] minimized cancer-cell kill versus normal-tissue survival, where both tissues were modeled by exponentional equations. Using the discrete-time state models, Kim et al. [3, 14] obtained a solution minimizing both the size of the tumor-cell population at the treatment's end and the excessive use of the drug; this method took into account the cell-cycle phase specificity of a drug, which was omitted by the others.

Although the discrete-time models may be convenient and easy to handle, they describe cell kinetics less accurately than the continuous-time state models, since cell cycling itself is a continuous process. The method of obtaining a solution to the continuous-time problem is quite different from that for the discrete-time problem. Using the continuous-time state models, this paper considers a method of (i) predicting the response of a cell population to treatment, and (ii) determining an optimal strategy in administering antitumor drugs.

This paper is organized as follows: Section II describes the continuous-time cell cycling model and the discrete-time measurement model; Section III shows computer simulations of the time-course behavior of a CHO cell population; and Section IV describes the optimization procedure and a numerical experiment on a CHO cell population for determining optimal dosage intervals. This numerical experiment should provide insights into the problem of generating good solutions to the cancer treatment scheduling problem.

II. CONTINUOUS-DISCRETE CELL-KINETIC MODELS

A cell population is appropriately modeled by a continuous state equation for the cell cycling process and by a discrete-time equation for cell population measurements.

2.1. *CONTINUOUS STATE MODEL OF CELL CYCLING PROCESS*

The cell cycling process of a tumor population under the effect of antitumor drug(s) can be modeled by a bilinear ordinary differential equation:

$$\dot{\mathbf{x}}(t) = F\mathbf{x}(t) + G\mathbf{x}(t)u(t), \qquad \mathbf{x}(t_0) = \mathbf{x}_0. \tag{1}$$

For convenience, a brief description of basic ideas underlying this equation is given as follows (see [7], [15] for further details). The cell cycle consists of four distinct phases (G_1, S, G_2, and M) and is divided into N equal intervals called age compartments. The physiological cell age distribution of a cell population is thus represented by an N-dimensional vector called the age state vector, the ith component of which represents the number of cells in the ith age compartment. Generally the state vector $\mathbf{x} \in R^n$ has additional components to include nonproliferating cells such as resting cells and dead cells. In this paper, the cell age state vector is partitioned as follows: the first N states describe the proliferating group, the next N states describe the resting cells, and the last state represents the dead cells (i.e. $n = 2N + 1$).

The variable $u(t)$ represents the external control function, namely the therapeutic function. Since the allowable dosage is always bounded (i.e., $0 \leqslant u(t) \leqslant u_{\max}$), one can assume $u(t) \in [0, 1]$ for all t without loss of generality. This implies that $u(t) = 0$ represents absence of the therapeutic agent, whereas $0 < u(t) \leqslant 1$ represents its presence. The expressions for the system matrices F and G are derived in two steps: first without therapy, to determine F, and then with therapy, to determine G.

The cell kinetics without chemotherapeutic effects, described by the matrix F, are formulated by applying the cell-conservation principle along with a study of the normal inflow and outflow mechanisms pertaining to each cell age state. This leads to the Poisson-type differential equations describing F as follows:

$$\begin{aligned}
\dot{x}_1(t) &= 2\delta_N x_N(t) - (\delta_1 + d_1 + f_1)x_1(t) + \gamma_1 x_{N+1}(t), \\
\dot{x}_2(t) &= \delta_1 x_1(t) - (\delta_2 + d_2 + f_2)x_2(t) + \gamma_2 x_{N+2}(t), \\
&\vdots \\
\dot{x}_N(t) &= \delta_{N-1} x_{N-1}(t) - (\delta_N + d_N + f_N)x_N(t) + \gamma_N x_{2N}(t), \\
\dot{x}_{N+1}(t) &= f_1 x_1(t) - (\gamma_1 + d_{N+1})x_{N+1}(t), \\
&\vdots \\
\dot{x}_{2N}(t) &= f_N x_N(t) - (\gamma_N + d_{2N})x_{2N}(t), \\
\dot{x}_n(t) &= \sum_{i=1}^{2N} d_i x_i(t) - k x_n(t),
\end{aligned} \tag{2}$$

where $\dot{x}_i(t)$ represents the instantaneous rate of change of cells in state i due to normal-cell cycling and cell transitions between proliferating and nonproliferating groups; δ_i, the probabilistic percentage of cells leaving the ith cell age compartment and entering the $(i+1 \bmod N)$th compartment, i.e. the cell aging rate; d_i, the probabilistic death rate in state i; f_i, the rate at which cells in state i of the proliferating group leave and become resting cells in the ith state, i.e. $x_{N+i}(t)$, of the nonproliferating group: γ_i, the rate at which cells from the ith nonproliferating state return to the ith proliferating-cell age compartment: and k, the dead-cell clearance rate. Experimental evidence has shown that resting cells are arrested at three cell-cycle stages: the early G_1 phase, the late G_1 phase, and the late $G_2 + M$ phase [16]. Therefore only three resting-cell compartments are used in the model, one for each cell cycle stage where this phenomenon occurs. This implies $x_{N+i}(t) = 0$ for all i except i-values corresponding to early G_1, late G_1, and late $G_2 + M$.

Similarly, the drug- or chemotherapeutic-dependent cell kinetics—namely, cell killing and cell blocking—represented by the matrix G are as follows:

$$\begin{aligned}
\dot{x}_1(t) &= \{(p_1\delta_1 - C_1)x_1(t) - 2p_N\delta_N x_N(t)\}u(t),\\
\dot{x}_2(t) &= \{(p_2\delta_2 - C_2)x_2(t) - p_1\delta_1 x_1(t)\}u(t),\\
&\vdots\\
\dot{x}_N(t) &= \{(p_N\delta_N - C_N)x_N(t) - p_{N-1}\delta_{N-1}x_{N-1}(t)\}u(t),\\
\dot{x}_{N+1}(t) &= -C_{N+1}x_{N+1}(t)u(t),\\
&\vdots\\
\dot{x}_{2N}(t) &= -C_{2N}x_{2N}(t)u(t),\\
\dot{x}_n(t) &= \sum_{i=1}^{2N} C_i x_i(t)u(t),
\end{aligned} \tag{3}$$

where $\dot{x}_i(t)$ represents the instantaneous rate of change in state i due to the presence of antitumor agents; C_i, the drug's killing rate per unit time in state i; and p_i, the fraction of cells blocked per unit time in state i which would normally age and migrate to state $(i+1 \bmod N)$ due to the drug effects. This cell blocking is called progression delay and occurs at certain specific cell-cycle stages, depending on the type of drugs applied. In agreement of experimental evidence, progression delay is assumed to occur at the G_1/S and G_2/M boundaries.

2.2. *CELL MEASUREMENT MODEL*

The cell age state previously defined cannot be measured directly but can be monitored indirectly by observing the cell size and the cell DNA content.

Presently, the flow-microfluorometry (FMF) technique offers large quantities of cell DNA-content data in a relatively short time with adequate statistical precisions [4–6]. The DNA-content distribution of a cell population can be related to the cell age distribution as follows. Cells in the G_1 phase will have a DNA content of one unit, whereas cells in both the G_2 and M phases will have a DNA content of two units. Cells in the S phase will have a DNA content between one and two units. Bearing this in mind, a new vector $\mathbf{z}(t_k)$, called the true DNA vector, was introduced by Kim et al. [7]. The ith component of $\mathbf{z}(t_k)$ represents the number of cells at time instant t_k with a DNA content $(i-0.5)/(M+1)$ units, where M is the dimension of $\mathbf{z}$. The true DNA vector is related to the cell age vector by

$$\mathbf{z}(t_k) = S\mathbf{x}(t_k), \tag{4}$$

where S is the transformation matrix that reorganizes the cell age state vector into the true DNA vector in terms of its DNA content instead of age. Let the experimental data acquired by FMF techniques be represented by $\mathbf{y}(t_k)$. The true DNA vector is related to the experimental DNA data as follows:

$$\mathbf{y}(t_k) = D\mathbf{z}(t_k), \tag{5}$$

where D is the matrix describing the dispersion in the FMF data due to errors in staining and device. Two methods are known for determining the form of the dispersion matrix: one approach fits a Gaussian curve to each of the two peaks in the distribution and a polynomial in between [17–18], and another fits a series of Gaussian curves, one for each discrete subinterval of DNA content, over the whole DNA distribution [15, 19].

III. COMPUTER SIMULATION

The model described in Section II was simulated and its time-course behavior was observed. The parameters used in this paper were inferred from those that were recursively estimated [11] using a discrete-time model. The FMF data used were taken on a Chinese-hamster-ovary (CHO) cell population. The original data[1] were reduced so that they would contain only 30 channels, the dimension of the FMF DNA vector. The mean generation time of the CHO cell population is known to be approximately 13 hours, and the ratio between the phase durations is 4:7:2. To keep the system order at a reasonable size, the number N of proliferating cell age states was taken to be 13. Hence the number of states in the G_1 phase is 4, the S phase 7, and the

[1] These data were obtained from Dr. Fried at the Sloan Kettering Cancer Institute, New York, New York.

1.00	1.00	1.00	1.00	0.00	0.00	0.00	0.00	0.00	0.00	0.00	0.00	0.00	1.00	1.00	0.00	0.00
0.00	0.00	0.00	0.00	0.78	0.00	0.00	0.00	0.00	0.00	0.00	0.00	0.00	0.00	0.00	0.00	0.00
0.00	0.00	0.00	0.00	0.22	0.56	0.00	0.00	0.00	0.00	0.00	0.00	0.00	0.00	0.00	0.00	0.00
0.00	0.00	0.00	0.00	0.00	0.44	0.33	0.00	0.00	0.00	0.00	0.00	0.00	0.00	0.00	0.00	0.00
0.00	0.00	0.00	0.00	0.00	0.00	0.67	0.11	0.00	0.00	0.00	0.00	0.00	0.00	0.00	0.00	0.00
0.00	0.00	0.00	0.00	0.00	0.00	0.00	0.78	0.00	0.00	0.00	0.00	0.00	0.00	0.00	0.00	0.00
0.00	0.00	0.00	0.00	0.00	0.00	0.00	0.11	0.67	0.00	0.00	0.00	0.00	0.00	0.00	0.00	0.00
0.00	0.00	0.00	0.00	0.00	0.00	0.00	0.00	0.33	0.44	0.00	0.00	0.00	0.00	0.00	0.00	0.00
0.00	0.00	0.00	0.00	0.00	0.00	0.00	0.00	0.00	0.56	0.22	0.00	0.00	0.00	0.00	0.00	0.00
0.00	0.00	0.00	0.00	0.00	0.00	0.00	0.00	0.00	0.00	0.78	0.00	0.00	0.00	0.00	0.00	0.00
0.00	0.00	0.00	0.00	0.00	0.00	0.00	0.00	0.00	0.00	0.00	1.00	1.00	0.00	0.00	1.00	0.00

(a)

0.0000	0.0000	0.0000	0.0000	0.0000	0.0000	0.0000	0.0000	0.0000	0.0000	0.0000
0.0000	0.0000	0.0000	0.0000	0.0000	0.0000	0.0000	0.0000	0.0000	0.0000	0.0000
0.0000	0.0000	0.0000	0.0000	0.0000	0.0000	0.0000	0.0000	0.0000	0.0000	0.0000
0.0000	0.0000	0.0000	0.0000	0.0000	0.0000	0.0000	0.0000	0.0000	0.0000	0.0000
0.0000	0.0000	0.0000	0.0000	0.0000	0.0000	0.0000	0.0000	0.0000	0.0000	0.0000
0.0000	0.0000	0.0000	0.0000	0.0000	0.0000	0.0000	0.0000	0.0000	0.0000	0.0000
0.0004	0.0000	0.0000	0.0000	0.0000	0.0000	0.0000	0.0000	0.0000	0.0000	0.0000
0.0219	0.0014	0.0001	0.0000	0.0000	0.0000	0.0000	0.0000	0.0000	0.0000	0.0000
0.2283	0.0343	0.0031	0.0002	0.0000	0.0000	0.0000	0.0000	0.0000	0.0000	0.0000
0.4987	0.2377	0.0474	0.0060	0.0006	0.0001	0.0000	0.0000	0.0000	0.0000	0.0000
0.2283	0.4533	0.2416	0.0604	0.0099	0.0013	0.0002	0.0000	0.0000	0.0000	0.0000
0.0219	0.2377	0.4156	0.2416	0.0723	0.0146	0.0024	0.0003	0.0000	0.0000	0.0000
0.0004	0.0343	0.2416	0.3836	0.2391	0.0829	0.0200	0.0039	0.0007	0.0001	0.0000
0.0000	0.0014	0.0474	0.2416	0.3562	0.2349	0.0920	0.0257	0.0058	0.0012	0.0002
0.0000	0.0000	0.0031	0.0804	0.2391	0.3325	0.2297	0.0995	0.0316	0.0082	0.0019
0.0000	0.0000	0.0001	0.0080	0.0723	0.2349	0.3117	0.2239	0.1056	0.0374	0.0110
0.0000	0.0000	0.0000	0.0002	0.0099	0.0829	0.2297	0.2933	0.2177	0.1104	0.0430
0.0000	0.0000	0.0000	0.0000	0.0006	0.0146	0.0920	0.2239	0.2770	0.2114	0.1142
0.0000	0.0000	0.0000	0.0000	0.0000	0.0013	0.0200	0.0995	0.2177	0.2625	0.2051
0.0000	0.0000	0.0000	0.0000	0.0000	0.0001	0.0024	0.0257	0.1056	0.2114	0.2493
0.0000	0.0000	0.0000	0.0000	0.0000	0.0000	0.0002	0.0039	0.0316	0.1104	0.2051
0.0000	0.0000	0.0000	0.0000	0.0000	0.0000	0.0000	0.0003	0.0058	0.0374	0.1142
0.0000	0.0000	0.0000	0.0000	0.0000	0.0000	0.0000	0.0000	0.0007	0.0082	0.0430
0.0000	0.0000	0.0000	0.0000	0.0000	0.0000	0.0000	0.0000	0.0000	0.0012	0.0110
0.0000	0.0000	0.0000	0.0000	0.0000	0.0000	0.0000	0.0000	0.0000	0.0001	0.0019
0.0000	0.0000	0.0000	0.0000	0.0000	0.0000	0.0000	0.0000	0.0000	0.0000	0.0002
0.0000	0.0000	0.0000	0.0000	0.0000	0.0000	0.0000	0.0000	0.0000	0.0000	0.0000
0.0000	0.0000	0.0000	0.0000	0.0000	0.0000	0.0000	0.0000	0.0000	0.0000	0.0000
0.0000	0.0000	0.0000	0.0000	0.0000	0.0000	0.0000	0.0000	0.0000	0.0000	0.0000
0.0000	0.0000	0.0000	0.0000	0.0000	0.0000	0.0000	0.0000	0.0000	0.0000	0.0000

(b)

FIG. 1. (a) Typical S-matrix. (b) Typical dispersion matrix (covariance = 0.08).

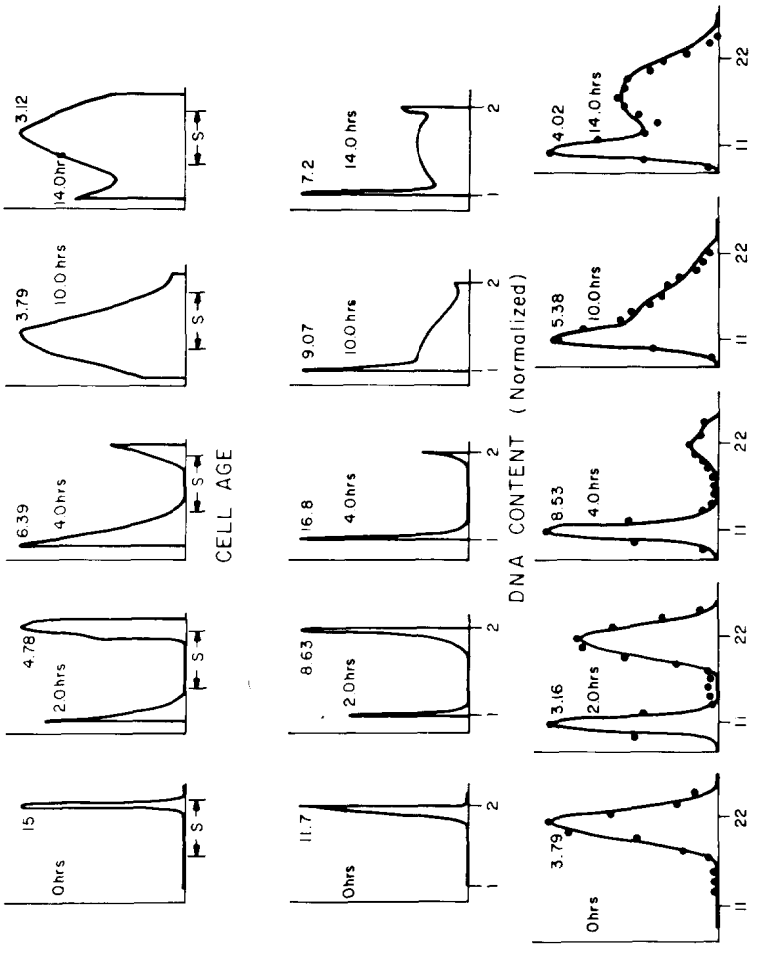

FIG. 2. Time-course behavior of a CHO-cell population without chemotherapy.

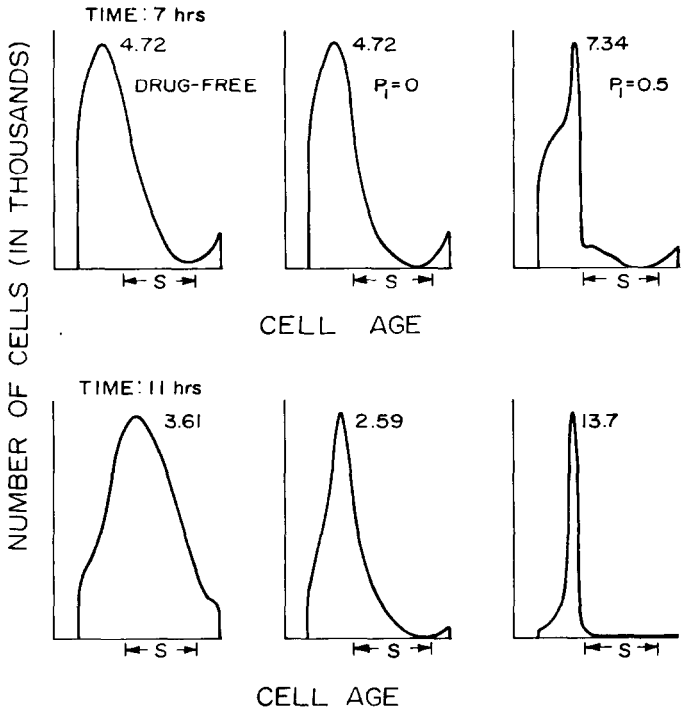

FIG. 3. (a) Cell age distribution following drug application at time 6 hours.

$G_2 + M$ phase 2. Here we have lumped the G_2 and M phases into one phase, the $G_2 + M$ phase. Since both phases contain the same amount of DNA content, the two phases are indistinguishable with the FMF data being used. The resulting cell age vector consists of 13 proliferating states, 3 resting states as discussed in [16], and the dead-cell age compartment. With this dimension for the system and dimension of 11 for $\mathbf{z}(t_k)$, Figure 1 illustrates the matrices S and D. The last column of S contains all zeros, since the effects of dead cells on the DNA data are generally assumed negligible. Note that using typical values of the cell-kinetic parameters, the system matrices F and G can be easily obtained from Equations (2) and (3).

The model was simulated for 14 hours with no control (drug-free environment). The plotted results for the cell age, true DNA, and computed FMF data are shown in Figure 2. Initially, most of the cells were congregated in the last S-phase compartment. As time passes, one can trace the progress of the cell population through the different cell phases. The experimental DNA (FMF) data points are superimposed on the simulated FMF distributions;

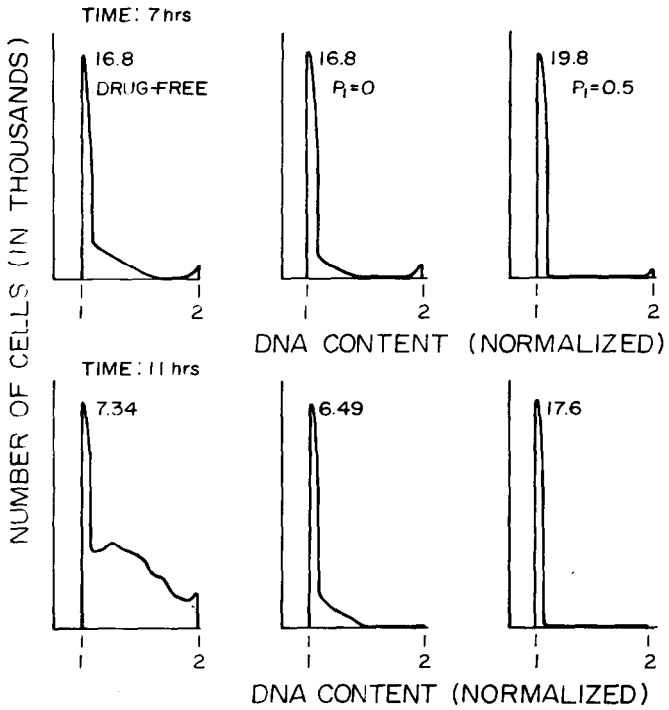

FIG. 3. (b) Cell DNA distribution following drug application at 6 hours.

these simulated distributions demonstrate consistency with the experimental ones.

The chemotherapeutic effects on the cell population are simulated next. Using the same parameter values and initial state, the time-course behavior of the cell population is simulated, but this time the drug is applied at time 6 hours. Another run with the cell blocking rate at the G_1/S boundary set to 0.5 shows the effect of progression delay at the G_1/S boundary. The cell age, true DNA, and computed DNA for these two cases are compared in Figure 3 for times of 7 and 11 hours.

IV. APPLICATION OF OPTIMAL-CONTROL THEORY FOR DERIVING CHEMOTHERAPY SCHEDULES

4.1. *OPTIMAL-CONTROL PROBLEM*

Optimal therapy is defined to be treatment which maximizes the probability of cure or, failing to achieve a cure, maximizes average survival times. To achieve either of these goals, any proposed treatment must maximize killing

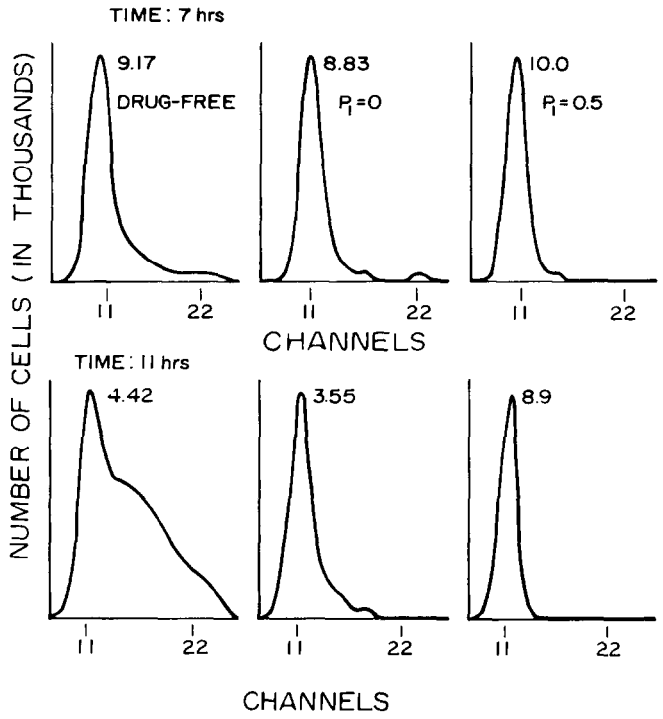

FIG. 3. (c) Cell FMF distribution following drug application at time 6 hours.

of cancer cells and simultaneously minimize toxicity to the host. Toxicity here implies damages to the critical normal cell populations such as bone-marrow cells and gastrointestinal tract cells. Any treatment must not reduce the size of such cell populations beyond the level necessary to maintain their important biological functions. Of course, this level must be determined by clinical and physical considerations.

Antitumor agents evoke two types of responses from both treated tumor and normal cell populations: lethality and delay in the normal transit through the mitotic cycle. These effects were modeled by a simple function in Section II. On the basis of this drug model, the optimal-control technique is used as a systematic tool for the best possible design of drug scheduling.

First, a performance index is chosen so the goodness of the treatment can be measured. The performance index used has the form

$$J = \mathbf{a}^T \mathbf{x}(t_f) + b \int_{t_0}^{t_f} u(w)\, dw, \tag{6}$$

where $\mathbf{a}$ and b are the weightings on the final cell age states and the control

respectively. This performance penalizes the final or remaining number of cancer cells at the end of the therapy period, but also penalizes excessive use of the drug. Since the allowable dosage is limited, the normalized control is bounded as follows:

$$0 \leq u(t) \leq 1 \qquad \text{for all } t \tag{7}$$

The problem is now to minimize the performance index (6) subject to the state equation (1) and the constraint (7). The Hamiltonian for this minimization is

$$H(t) = bu(t) + \mathbf{p}^T(t)[F\mathbf{x}(t) + G\mathbf{x}(t)u(t)], \tag{8}$$

where $\mathbf{p}$ is the costate vector satisfying

$$\dot{\mathbf{p}}(t) = -\frac{\delta H}{\delta \mathbf{x}}. \tag{9}$$

Application of the maximum principle [20] immediately shows that the form of the optimal control is a bang-bang type:

$$u(t) = \operatorname{sgn}\{b + \mathbf{p}^T(t)G\mathbf{x}(t)\} \tag{10}$$

where sgn represents the sign of the quantity in braces. This quantity is called the switching function and denoted by $s(t)$. When $s(t)$ crosses zero, the control switches state: from full on to full off or vice versa. The final condition on the costate is computed from the transversality conditions,

$$\mathbf{p}(t_f) = \frac{\delta J(\mathbf{x}(t_f))}{\delta \mathbf{x}(t_f)}. \tag{11}$$

The state and costate differential equations, (1) and (9), along with the final condition on the costate and the initial condition on the state, completely describe a two-point boundary-value problem (TPBVP). Analytical solutions to TPBVPs are usually impossible to obtain in all but very simple situations, and thus numerical techniques are sought. This optimal-control problem, with its bilinear form, meets the requirements of one algorithm available: the switching-time variational method (STVM) [21]. This method incorporates a modified gradient scheme to successively compute an approximate solution to the optimal-bilinear-control problem.

4.2. *COMPUTER-SIMULATION RESULTS FOR OPTIMAL TREATMENTS*

To demonstrate the utility of the optimal-control method, we simulated the results of applying the STVM algorithm to the optimal-control problem with a therapy period of 6 hours. The system parameters were varied and their effects on the optimal control noted. For convenience, only phase-specific drugs that affect only cells in the S phase are considered in this simulation.

Comparison of Optimal and Suboptimal Treatments. The optimal solution to the TPBVP was found to contain two switching times. This optimal therapy was compared with several suboptimal dosage schedules listed in Table 1, the optimal schedule being listed first. The duration of the control was kept constant in each case, though that was not necessary. In the second case, the number of cells increased because the drug was not administered long enough initially. Therefore more cells would survive and reproduce. The fact that the drug was present for a longer time near the end of the treatment schedule had little effect on the cancer-cell population, since the majority of the cells had not aged enough to reach the S phase. The cell age, true DNA, and computed DNA distributions for the first two entries of Table 1, an optimal and a suboptimal solution, are shown in Figures 4 and 5. If the control is initially on for its maximum duration of 2.81 hours, the number of CHO cells remaining at the end of the treatment schedule is more than the optimal number, even though it is less at time 2.81 hours. This can be explained as follows. The first 1 to 2 hours of the drug application kills the cells in the late S phase. But the last hour or so is wasted because there are essentially no cells remaining in the S phase. It would be more beneficial to postpone the application of the remaining dose until the cells had reached the S phase. The fourth case can be explained in a similar manner. In the last

TABLE 1

A Comparison between Optimal and Suboptimal Cancer Treatment Schedules[a]

Initial control $u(0)$	Final switching vector $\mathbf{T}_f$	Performance index J_f
+1	1.7, 4.89	15,202
+1	1.0, 4.19	16,120
+1	2.81	17,185
+1	0.5, 3.0, 4.0, 4.69	18,573
−1	2.9, 4.9, 5.19	24,108
−1	3.19	24,377

[a]The first row is the optimal cancer-treatment schedule. The subscript f represents the final time.

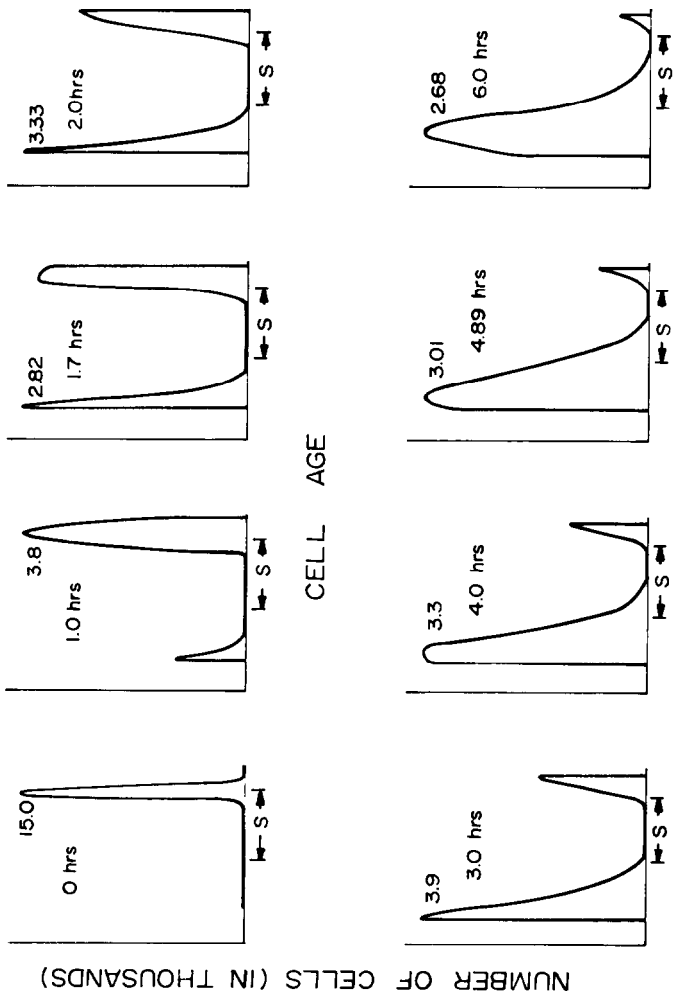

FIG. 4. (a) Time-course behavior of cell age distribution under optimal treatment.

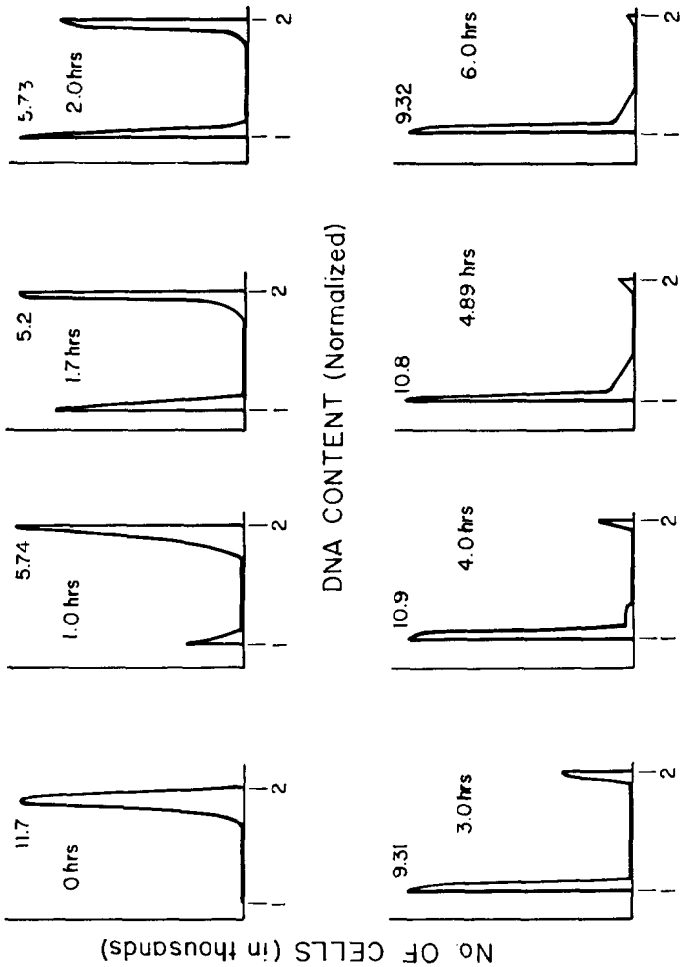

FIG. 4. (b) Time-course behavior of cell DNA distribution under optimal treatment.

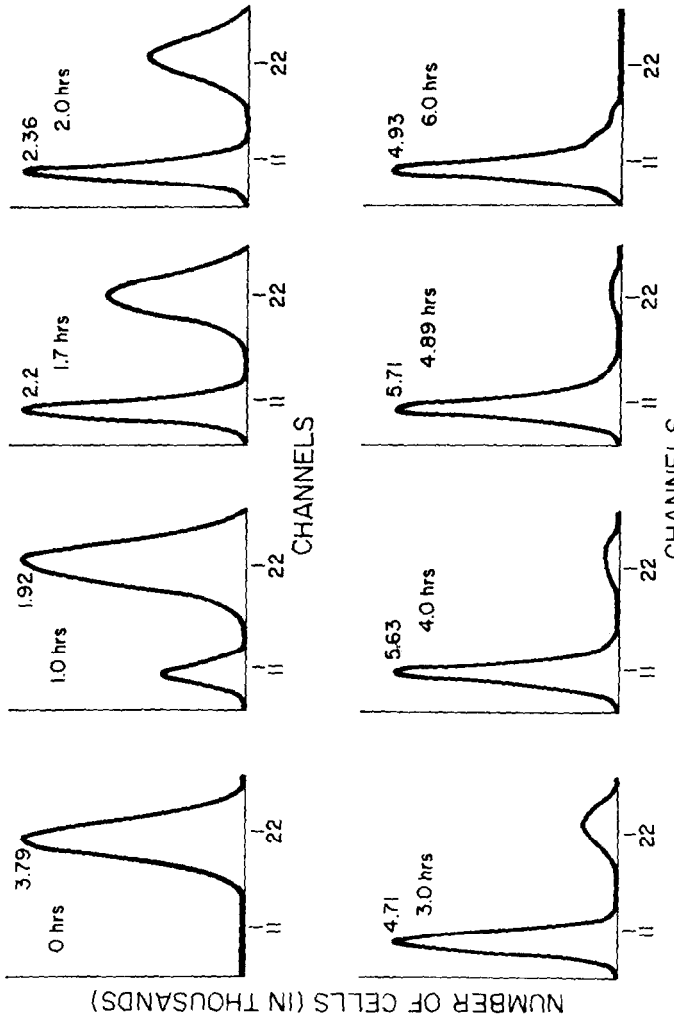

FIG. 4. (c) Time-course behavior of cell FMF distribution under optimal treatment.

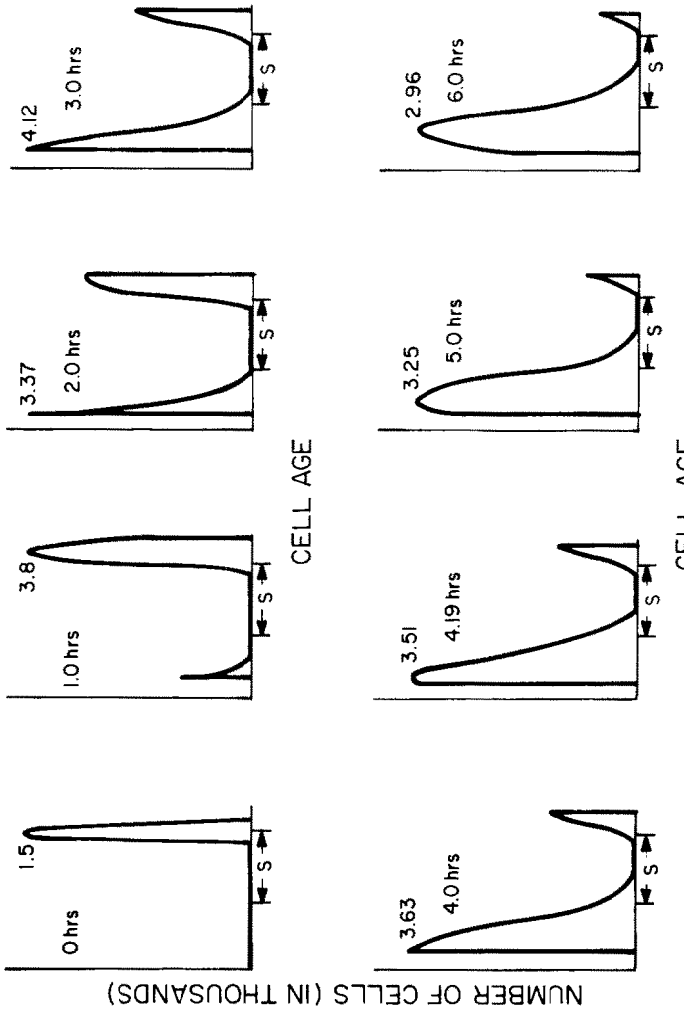

FIG. 5. (a) Time-course behavior of cell age distribution under suboptimal treatment.

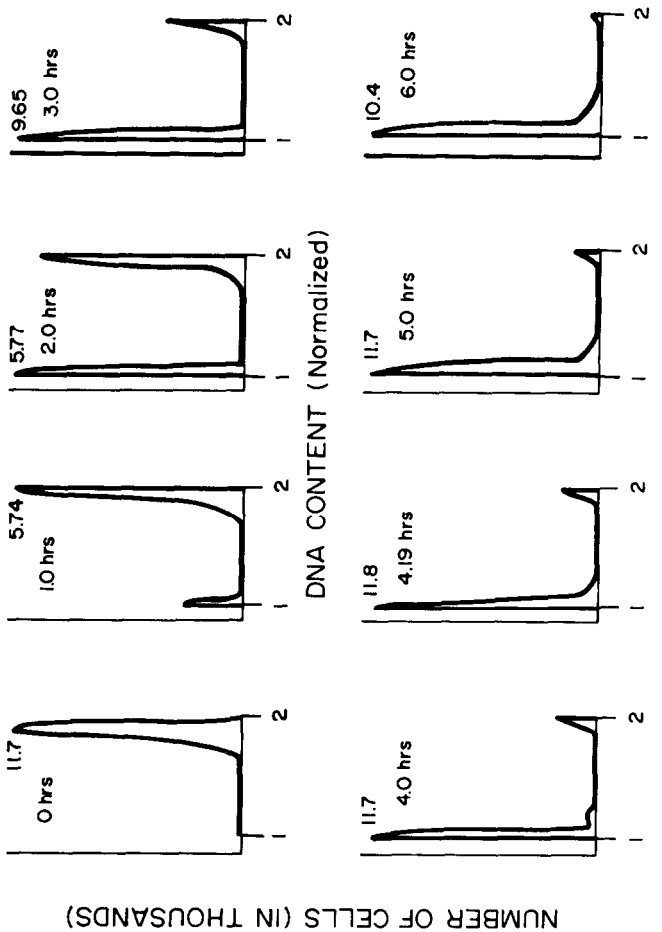

FIG. 5 (b) Time-course behavior of cell DNA distribution under suboptimal treatment.

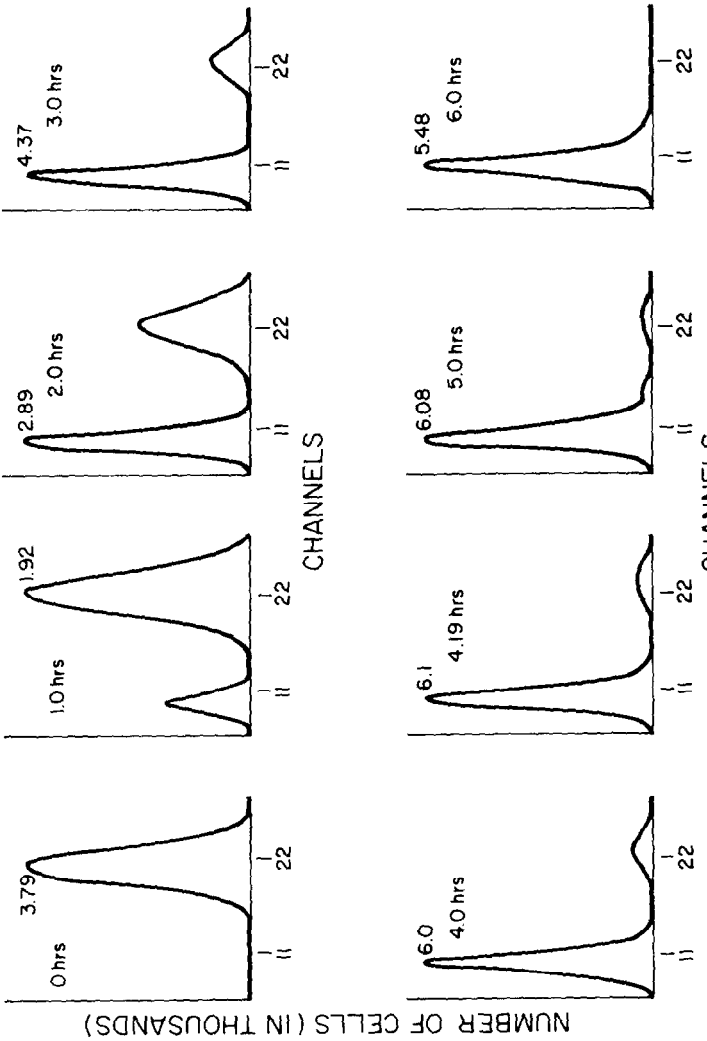

FIG. 5. (c) Time-course behavior of cell FMF distribution under suboptimal treatment.

two cases the control was initially off, so most of the cells were able to divide, thereby increasing the CHO cell population significantly. The drug applied at later times had little effect upon the cell population, since most of the cells had not reached the S phase for this treatment period.

Performance-Index Weighting Measurements. The weighting factors **a** and b of the performance index in (6) were changed and their effect noted. It was found that the magnitude of the weightings had little effect on the control. The main contributor to the final result is the ratio between **a** and b. If the weighting on the control was increased, the duration of the control or drug was reduced, causing an increase in the number of CHO cells remaining at the end of the therapy period. The opposite was true if the weighting on the control was decreased. Similiar results were obtained if the weighting on the CHO cell's final state was varied. The results of changing the weighting on the control while keeping the other variables constant is tabulated in Table 2. It can been seen that as the weighting on the control is reduced, its duration increases and the number of CHO cells remaining diminishes.

Effects of Different Initial Conditions. The initial state of the cell population plays an important role in the determination of the treatment schedule, as we have already seen. To show this the initial state of the cell population is varied and the resulting optimal sequence analyzed. A listing of the different initial conditions are found in Table 3, and the corresponding treatment period is illustrated in Table 4. For initial condition I, the majority of the cells are in the second compartment of the G_1 phase. These cells will migrate to the S phase in approximately 3 hours. The optimal control indicates that

TABLE 2

The Effects of Different Weightings on the Control[a]

N^*[b]	Cost of control	Cells remaining	Wt. on control	T_f[c]
1	3198	10,463	6000	5.47
1	3925	8,226	4000	5.02
1	3428	6,085	2000	4.29
1	2402	5,081	1000	3.60
1	1518	4,620	500	2.96
1	762	4,364	200	2.19
2	446	4,274	100	0.087, 1.62

[a] The weighting **a** on the final cell age states is held constant at 1.0.
[b] Optimal number of switchings
[c] Final switching time vector

TABLE 3

Different Initial Conditions Used in the Simulation

Init. cond.	x_{11}	x_{12}	x_{13}	x_{14}	x_{s1}	x_{s2}	x_{s3}	x_{s4}	x_{s5}	x_{s6}	x_{s7}	x_{21}	x_{22}
I	20	15k	0	0	0	167	60	0	41	14	57	0	0
II	20	10	0	0	15k	167	60	0	41	14	57	0	0
III	20	10	0	0	0	167	60	15k	41	14	57	0	0
IV	20	10	0	0	0	167	60	0	41	15k	57	0	0
V	20	10	0	0	0	167	60	0	41	14	15k	0	0
VI	20	10	0	0	0	167	60	0	41	14	57	15k	0
VII	20	10	0	0	0	167	60	0	41	14	57	0	15k
VIII	15k	10	0	0	0	167	60	0	41	14	57	0	0

the drug should be applied at time 3.59 hours and left on for the remainder of the treatment period, while the cell population is distributed mainly in the S phase. For the next three cases, namely II, III, and IV, the bulk of these cell populations is somewhere in the S phase. The drug is applied immediately, since the cancer cells are maximally susceptible to the drug. As expected, when the majority of the cells at the initial time occur later in the S phase, the duration of the drug application is reduced and the final cancer-cell population increases. For cases VI and VII, the number of remaining cells is large, since most of the cells are able to divide. The resulting drug schedules are acceptable; as the time that it takes the bulk of the cell population to reach the S phase decreases, the time of the drug application also decreases. The final case examined, case VIII, is similar to case I.

TABLE 4

The Effects of Different Initial Conditions on the System

Init. cond.	N^{*a}	J^{*b}	T_f^c	$u(0)$	Cells remaining	Cost of control
I	1	7,483	3.59	−1	5.073	2410
II	1	4,437	3.06	+1	1,377	3060
III	1	5,409	2.96	+1	2,449	2960
IV	2	9,667	2.4, 5.86	+1	7,127	2540
VI	1	23,659	4.44	−1	22,099	1560
VII	1	20,681	3.97	−1	18,651	2030
VIII	1	9,403	4.04	−1	7,443	1960

[a] Optimal number of switchings.
[b] Optimal final cost.
[c] Final switching time vector.

It has been shown that the initial state of the CHO-cell population drastically effects the optimal treatment schedule. It must be remembered that the therapy period used here is 6 hours. This does not provide enough time for the cell population to complete even one cycle. It does provide, though, some insight into the effects of the initial state upon the drug administration period. From these results, it would be ideal to accumulate all cancer cells in the late G_1 phase, release the block, and then apply the drug soon after so that its effects are maximally felt in the shortest time frame possible.

Effects of the System Matrices Parameters. The continuous-time model's parameters were altered in a number of ways, tabulated in Table 5, from the original parameters i.e., the first entry of the table. The resulting optimal therapy schedules are shown in Table 6. The first parameter varied was the progression delay at the G_1/S transition boundary. With P_1 set 0.5, cells will accumulate in the last G_1-phase-cell age state while the drug is present. Therefore the drug should not be applied until more of the cells are actually

TABLE 5

Parameter Values Used for Stimulation[a]

Case	C_s	δ_1	δ_s	δ_2	p_1
I	.8	.8	.8	.8	.0
II	.8	.8	.8	.8	.5
III	.8	.9	.9	.9	.0
IV	.8	.6	.6	.6	.0
V	.8	.4	.4	.4	.0
VI	.8	.8	.4	.8	.0
VII	.5	.8	.8	.8	.0
VIII	.3	.8	.8	.8	.0
IX	.9	.8	.8	.8	.0

Parameters held constant

$d_1 = 0.01$	$\gamma_1 = 0.02$
$d_s = 0.01$	$\gamma_2 = 0.02$
$d_2 = 0.01$	$\gamma_3 = 0.0$
$d_m = 0.0$	$f_1 = 0.02$
$C_1 = 0.0$	$f_2 = 0.0$
$C_2 = 0.0$	$f_3 = 0.0$
$C_m = 0.0$	$p_2 = 0.0$
$k = 0.0$	

[a]Subscripts indicate phases; e.g. C_s = cell-killing rate by drug(s) in phase S.

TABLE 6

The Effects of Different Parameter Values on the Cell System

Case	N^{*a}	J^{*b}	$\mathbf{T}_f^c$
I	1	7,482	3.60
II	1	8,271	4.05
III	1	6,851	3.41
IV	1	9,458	3.98
V	1	12,176	4.53
VI	1	7,305	3.66
VII	1	9,347	3.32
VIII	1	11,473	3.31
IX	1	7,064	3.70

[a]Optimum number of switchings.
[b]Optimal final cost
[c]Final switching-time vector.

in the S phase, since once it is administered, the inflow of cells into the S phase will be diminished severely. In order to study the full effect of this parameter, the treatment period will have to be lengthened.

The variable δ is successively reduced in cases III, IV, and V. The result is to apply the drug at later times, because less cells will have reached the S phase. Case VI is similar to I except that the aging-rate variable δ was less during the S phase and produced little effect. The last three cases deal with the toxicity of the drug to the cancer population in the S phase. It was determined that the drug with the highest toxicity to the CHO-cell population should be administered for the shortest time.

V. CONCLUSION

The growth of a tumor population under the effects of antitumor drugs has been represented by a continuous-time, bilinear state model. Using this model, the time-course behavior of a CHO-cell population was simulated for a period of 14 hours with favorable results. The model was also used to determine an optimal cancer treatment strategy for various initial conditions and cell-kinetic parameter values. The results of this study indicate that such a model is highly valuable; there is great potential in using it to predict systematically high cancer kill rates with lower toxicity to the patients.

There are, however, several ways the present work can be improved. One is to improve the drug model; in particular, drug kill rates are only partly linear and often mostly exponential. The change of the drug model will in turn require reformulation of the optimal-control problem and will change the nature of the solution space, as the dosage level at any instant will be allowed to vary (i.e., we no longer have a bang-bang control policy). Another

way is to extend the treatment period of in computer simulation beyond 6 hours, the maximum time the STVM program was able to produce acceptable results. For times greater than this, the overall performance index was reduced but the solution did not converge to the form predicted by the STVM. This convergence problem for longer treatment periods is caused by the propagation of numerical roundoff errors through the age states and the costates when they are integrated forward and backward, respectively. This numerical problem should be solved by special techniques or by using superaccurate computer (e.g. precision >64 bits) to handle longer periods than 6 hours.

REFERENCES

1 J. Aroesty, T. Lincoln, N. Shapiro, and G. Boccia, Tumor growth and chemotherapy: Mathematical methods, computer simulations, and experimental formulations, *Math. Biosci.* 17:243–300 (1973).

2 P. C. Steward and G. M. Hahn, The application of age response functions to the optimization of treatment schedules, *Cell Tissue Kinet.* 4:279–291 (1971).

3 K. Bahrami and M. Kim, Optimal control of multiplicative control systems arising from cancer therapy, *IEEE Trans. Automatic Control* AC-20(4):537–542 (Aug. 1975).

4 L. A. Kamentsky, M. R. Melamed, and H. Derman, Spectrophotometer: New instrument for ultrarapid cell analysis, *Science* 150:630 (1965).

5 P. M. Kramer, L. L. Devan, H. A. Crissman, and M. A. Van Dilla, The paradox of DNA constancy in heteroploidy, *Adv. Cell Mol. Biol.* 2:47–108 (1972).

6 M. A. Van Dilla, T. T. Trujillo, P. F. Mullaney, and J. R. Coulter, Cell microfluorometry: A method for rapid fluorescence measurement, *Science* 113:1213–1214 (1969).

7 M. Kim, K. Bahrami, and K. Woo, A discrete-time model for cell-age, size, and DNA distributions of proliferating cells, and its applications to the movement of the labeled cohort, *IEEE Trans. Biomedical Engrg.* 21:387–398 (1974).

8 G. Hahn, State vector description of the proliferation of mammalian cells in tissue culture, *J. Biophys.* 6:275–290 (1966).

9 M. Kim, K. G. Shin, and S. Perry, Estimation of cell kinetic parameters from flow microfluorometry, *Math. Biosci.* 38:77–89 (1978).

10 M. Kim, B. C. Wheeler, and S. Perry, Quantitative description of cell cycle kinetics under chemotherapy utilizing flow cytometry, *Cell Tissue Kinet.* 11:497–512 (1978).

11 K. G. Shin and M. Kim, Recursive least squares estimation of cell kinetic parameters using sequential measurements of cell DNA contents, *IEEE Trans. Systems Man Cybernet.* SMC-10(12):861–873 (Dec. 1980).

12 G. W. Swan and T. L. Vincent, Optimal control analysis in the chemotherapy of IgG multiple myeloma, *Bull. Math. Biol.* 39:317–337 (1977).

13 K. J. Almquist and H. T. Banks, A theoretical and computational method for determining optimal treatment schedules in fractionated radiation therapy, *Math. Biosci.* 29:159–179 (1976).

14 M. Kim, K. B. Woo, and S. Perry, A quantitative approach to the design of antitumor drug dosage schedule via cell cycle kinetics and system theory, *Ann. Biomed. Engrg.* 5:12–33 (1977).

15 J. W. Gray, Cell-cycle analysis of perturbed cell populations: Computer simulation of sequential DNA distributions, *Cell Tissue Kinet.* 9:499–516 (1976).
16 S. Gelfant, A new concept of tissue and tumor cell proliferation, *Cancer Research* 37:3845–3862 (Nov. 1977).
17 H. Baisch, W. Göhde, and W. A. Linden, Analysis of PCP-data to determine the fraction of cells in the various phases of cell cycle, *Rad. and Environm. Biophys.* 13:31–39 (1975).
18 P. N. Dean and J. H. Jett, Mathematical analysis of DNA distributions derived from flow microfluorometry, *J. Cell Biol.* 60:523–527 (1974).
19 J. Fried, Method for the quantitative evaluation of data from flow microfluorometry, *Comput. and Biomed. Research* 9:263–276 (1976).
20 A. P. Sage, *Optimal Systems Control*, Prentice-Hall, Englewood Cliffs, N.J., 1968.
21 R. R. Mohler, *Bilinear Control Processes*, Academic, New York, 1973.